



The Antibacterial Effects of New N-Alkylpyridinium Salts on Planktonic and Biofilm Bacteria

Michaela Hymanova^{1,2}, Saša Terlep³, Aneta Markova^{1,4}, Lukáš Prchal¹, Iztok Dogsa⁵, Lenka Pulkrabkova^{1,4}, Marketa Benkova¹, Jan Marek^{1,2} and David Stopar^{5*}

¹ Biomedical Research Centre, University Hospital Hradec Kralove, Hradec Kralove, Czechia, ² Department of Epidemiology, Faculty of Military Health Sciences, University of Defence in Brno, Brno, Czechia, ³ Fotona d.o.o., Ljubljana, Slovenia, ⁴ Department of Toxicology and Military Pharmacy, Faculty of Military Health Sciences, University of Defence in Brno, Brno, Czechia, ⁵ Department of Microbiology, Biotechnical Faculty, University of Ljubljana, Ljubljana, Slovenia

OPEN ACCESS

Edited by:

Fabian Cieplik,
University Medical Center
Regensburg, Germany

Reviewed by:

Biao Ren,
Sichuan University, China
Cesar de la Fuente-Nunez,
University of Pennsylvania,
United States

*Correspondence:

David Stopar
david.stopar@bf.uni-lj.si

Specialty section:

This article was submitted to
Antimicrobials, Resistance
and Chemotherapy,
a section of the journal
Frontiers in Microbiology

Received: 18 June 2020

Accepted: 28 September 2020

Published: 20 October 2020

Citation:

Hymanova M, Terlep S, Markova A, Prchal L, Dogsa I, Pulkrabkova L, Benkova M, Marek J and Stopar D (2020) The Antibacterial Effects of New N-Alkylpyridinium Salts on Planktonic and Biofilm Bacteria. *Front. Microbiol.* 11:573951. doi: 10.3389/fmicb.2020.573951

An increasing microbial resistance to known antibiotics raises a demand for new antimicrobials. In this study the antimicrobial properties of a series of new N-Alkylpyridinium quaternary ammonium compounds (QACs) with varying alkyl chain lengths were evaluated for several nosocomial pathogens. The chemical identities of the new QACs were determined by NMR, LC-MS, and HRMS. All the planktonic bacteria tested were susceptible to the new QACs as evaluated by MIC and MBC assays. The antimicrobial effect was most pronounced against *Staphylococcus aureus* clinical isolates. Live/dead staining CLSM was used to test the effectiveness of the QACs in biofilms. The effectiveness was up to 10-fold lower than in the plankton. When QACs were used as irrigants in Er:YAG – SSP photoacoustic steaming, their effectiveness significantly increased. The combined use of irrigants and photoacoustic streaming increased biofilm removal from the surface and increased the killing rate of the cells remaining on the surface. This may allow for a shorter chemical exposure time and lower dosage of QACs used in applications. The results demonstrate that the new QACs have potential to be applied as antibacterial compounds effective against planktonic and biofilm bacteria as well as irrigants in removal of difficult-to-reach biofilms.

Keywords: antimicrobial activity, quaternary ammonium salts, bacteria, biofilm, photoacoustic irrigation

INTRODUCTION

Infectious diseases caused by pathogenic bacteria are a threat to public health all over the world (Courvalin, 2016; Watkins, 2018). A high prevalence of resistance against known antibacterial agents aggravates the situation. For instance, many nosocomial pathogens such as *Pseudomonas aeruginosa*, *Staphylococcus aureus*, *Escherichia coli*, *Klebsiella pneumoniae*, and *Enterococcus faecalis* are resistant to known antimicrobials and are difficult to treat (Khan et al., 2017). There is an urgent need to develop new antibacterial agents that will replace those to which bacteria have developed resistance. In particular the new antibacterial agents should have good activity against biofilm bacteria which are typically more resistant and are more difficult to remove from surfaces (Ceri et al., 1999; Olson et al., 2002).

Quaternary ammonium compounds (QACs), are widely used in medicine. They have proven antimicrobial properties, have low toxicity, and are minimally irritating (Gerba, 2015). They are most effective against Gram positive bacteria, but are also effective against Gram negative bacteria, viruses and biofilms (Jennings et al., 2014; Gerba, 2015). QACs can be used in antibacterial formulations or incorporated into medical products, such as composite materials or acrylic resins, or adhesive systems and endodontic dental materials, where their antimicrobial activity against *Streptococcus mutans*, *E. faecalis* or other bacteria decreases the occurrence of secondary caries infection (Zhang et al., 2018).

In difficult-to-reach biofilm infections chemical treatments are sometimes combined with physical or mechanical co-treatment methods to increase their effectiveness. For example, in a dental root canal procedure chemical antibacterial treatment (i.e., sodium hypochlorite) is combined with root irrigation. However, sodium hypochlorite is toxic and is not suitable for certain medical applications (i.e., in dental implant related peri-implant mucositis and peri-implantitis). The traditional method of irrigation using a syringe with a needle often fails because of the limited irrigant flow and its ability to reach distant areas (Boutsioukis et al., 2010). Various new irrigant activation techniques have been suggested to improve biofilm removal (Kurzmann et al., 2019). The non-contact Er:YAG photoacoustic streaming with Super Short Pulses (SSP, 50 μ s) has been a very successful method of removing biofilms from the dental root system for many years (Olivi et al., 2014; Akcay et al., 2017; Lukač and Jezeršek, 2018; Kurzmann et al., 2019). Er:YAG photoacoustic irrigation causes biofilm mechanical debridement by turbulent movement of fluid irrigant, and at the same time the chemical action of the irrigant itself significantly improves biofilm removal. The problem with irrigation techniques is that many of currently used irrigants in dentistry are toxic in high concentrations (Clarkson and Moule, 1998; Zehnder, 2006). It would therefore be beneficial if new antibacterial irrigants (e.g., QACs) with lower toxicity were available, especially for irrigation in presence of vital tissue. The use of QACs for photoinduced irrigation treatment of biofilms has not been tested yet.

In this study new QACs were evaluated for their efficiency as irrigant and antibacterial compounds against plankton and biofilm. Antibacterial effects were tested on clinical isolates of nosocomial pathogens including *S. aureus*, *Staphylococcus epidermidis*, *E. faecalis*, *E. coli*, and *K. pneumoniae*. For laboratory testing and irrigation experiments non-pathogenic strain of *E. faecalis* was used. The antibacterial effect was probed either by chemical treatment or a combination of chemical and Er:YAG irrigation methods. The chemical identity of the new QACs was determined by NMR, LC-MS, HRMS. The antibacterial activity of QACs was measured with MIC and MBC assays. The results suggest that new QACs have a good potential as antibacterial compounds effective against planktonic and biofilm bacteria, and also as irrigants in laser-assisted removal of biofilms.

MATERIALS AND METHODS

Chemistry

General Information

The preparation of 1-Alkylpyridinium derivatives (**A**₁₂, **A**₁₄, **A**₁₆) and 3-alkyl-1-(2-hydroxyethyl)imidazolium (**C**₁₂, **C**₁₄, **C**₁₆) derivatives with appropriate alkyl chain length ($-C_{12}H_{25}$; $-C_{14}H_{29}$; $-C_{16}H_{33}$) has been described previously (Marek et al., 2010; Soukup et al., 2020). The series of 1-alkyl-3-chloropyridinium derivatives (**B**₁₂, **B**₁₄, **B**₁₆) was prepared for the first time in this study by refluxing 3-chloropyridine (18 mM) with the appropriate alkyl bromide (45 mM) in acetonitrile (50 ml) for 96 h. The acetonitrile was evaporated and the crude product purified by recrystallization several times from diethyl ether. Alkyl bromides and 3-chloropyridine were purchased from Sigma-Aldrich (Prague, Czechia) and used without further purification. Acetonitrile was purchased from VWR (Prague, Czechia). The reaction progress was monitored by thin layer chromatography (TLC) on aluminum sheets with silica gel 60 F₂₅₄ purchased from Merck (Prague, Czechia) in a mobile phase of methanol: ethyl acetate: ammonia solution = 3: 1: 0.1. Detection was carried out with ultraviolet light (254 nm) or with KMnO₄ solution (1% aq. sol.). ¹H NMR and ¹³C NMR spectra were recorded in CDCl₃ at ambient temperature on a Varian S500 spectrometer (499.87 MHz for ¹H and 125.71 MHz for ¹³C). Chemical shifts, δ , are given in parts per million (ppm), and spin multiplicities are given as s (singlet), d (doublet), dd (doublet of doublets), dt (doublets of triplets), t (triplet) or m (multiplet). Coupling constants, *J*, are expressed in hertz (Hz). For ¹H, δ is relative to CDCl₃ ($\delta = 7.26$) and for ¹³C relative to CDCl₃ ($\delta = 77.00$). Melting points were determined by melting point apparatus – Stuart SMP30 (Eaton, United Kingdom) – and were uncorrected.

LC-MS Analysis

High performance liquid chromatography (HPLC) coupled with mass spectrometry (MS) detection was performed to determine the identity and purity of the prepared compounds. The system used in this study was a Dionex Ultimate 3000 UHPLC: RS Pump, RS Column Compartment, RS Autosampler, Diode Array Detector, Chromeleon (version 7.2.9 build 11323) software (Thermo Fisher Scientific, Germering, Germany) with Q Exactive Plus Orbitrap mass spectrometer with Thermo Xcalibur (version 3.1.66.10.) software (Thermo Fisher Scientific, Bremen, Germany). Detection was performed by mass spectrometry in positive mode. The settings for the heated electrospray source were: spray voltage 3.5 kV; capillary temperature: 300°C; sheath gas: 55 arbitrary units; auxiliary gas: 15 arbitrary units; spare gas: 3 arbitrary units; probe heater temperature: 250°C; max spray current: 100 μ A; S-lens RF Level: 50. High resolution mass spectra (HRMS) and sample purities were obtained by HPLC-MS gradient method. A C18 column was used (Phenomenex Kinetex EVO C18, 3 \times 150 mm, 2.6 μ m, Phenomenex, Japan). Mobile phase A was ultrapure water of ASTM I type (resistivity 18.2 M Ω .cm at 25°C) prepared by Barnstead Smart2Pure 3 UV/UF apparatus (Thermo Fisher Scientific, Bremen, Germany) with 0.1% (v/v) formic acid;

mobile phase B was acetonitrile (MS grade, Honeywell Sigma-Aldrich, Germany) with 0.1% (v/v) of formic acid. The flow was constant at 0.4 mL/min. The method began with 1 min of isocratic flow of 5% B, followed by gradient flow of B rising to 100% B in 3 min, followed by constant flow of 100% B for 1 min. The composition then went back to 5% B and equilibrated for 5 min. Total run time was 10 min. The samples were dissolved in methanol (LC-MS grade, Fluka Sigma-Aldrich, Steinheim, Germany) at a concentration of 1 mg/mL and sample injection was 1 μ L. Purity was determined by UV at 254 nm. HRMS was determined by total ion current spectra from the mass spectrometer.

NMR and HRMS Data

1-dodecyl-3-chloropyridinium bromide (B₁₂)

¹H NMR (500 MHz, methanol-d₄) δ 9.37 (t, J = 1.8 Hz, 1H, ArH), 9.06 (dt, J = 6.0, 1.2 Hz, 1H, ArH), 8.73–8.67 (m, 1H, ArH), 8.14 (dd, J = 8.5, 6.1 Hz, 1H, ArH), 4.71–4.64 (m, 2H, CH₂), 2.10–2.01 (m, 2H, CH₂), 1.48–1.24 (m, 18H, 9 \times CH₂), 0.90 (t, J = 7.0 Hz, 3H, CH₃).

¹³C NMR (126 MHz, CD₃OD) δ 146.67, 145.53, 144.72, 137.01, 130.04, 63.61, 33.05, 32.42, 30.71, 30.61, 30.47, 30.44, 30.09, 27.16, 23.71, 14.43.

ESI-MS: m/z 282.20 [M⁺] (calc. for [C₁₇H₂₉ClN⁺] 282.20).

1-tetradecyl-3-chloropyridinium bromide (B₁₄)

¹H NMR (500 MHz, chloroform-d) δ 9.70–9.65 (m, 2H, ArH), 8.48 (dd, J = 7.8, 1.8 Hz, 1H, ArH), 8.25 (dd, J = 8.5, 6.0 Hz, 1H, ArH), 5.10 (t, J = 7.5 Hz, 2H, CH₂), 2.09–1.99 (m, 2H, CH₂), 1.45–1.14 (m, 22H, 11 \times CH₂), 0.86 (t, J = 6.8 Hz, 3H, CH₃).

¹³C NMR (126 MHz, CDCl₃) δ 144.97, 144.12, 143.75, 135.65, 129.16, 62.35, 31.98, 31.82, 29.58, 29.54, 29.51, 29.44, 29.27, 29.25, 29.01, 25.97, 22.59, 14.03.

ESI-MS: m/z 310.23 [M⁺] (calc. for [C₁₉H₃₃ClN⁺] 310.23).

1-hexadecyl-3-chloropyridinium bromide (B₁₆)

¹H NMR (500 MHz, chloroform-d) δ 9.68 (d, J = 6.0 Hz, 1H, ArH), 9.63 (t, J = 1.7 Hz, 1H, ArH), 8.48 (dd, J = 8.4, 2.0 Hz, 1H, ArH), 8.24 (dd, J = 8.5, 6.0 Hz, 1H, ArH), 5.11 (t, J = 7.5 Hz, 2H, CH₂), 2.09–1.99 (m, 2H, CH₂), 1.46–1.11 (m, 26H, 13 \times CH₂), 0.86 (t, J = 6.9 Hz, 3H, CH₃).

¹³C NMR (126 MHz, CDCl₃) δ 144.98, 144.16, 143.70, 135.67, 129.15, 62.41, 31.98, 31.85, 29.63, 29.58, 29.54, 29.46, 29.29, 29.03, 25.99, 22.61, 14.05.

ESI-MS: m/z 338.26 [M⁺] (calc. for [C₂₁H₃₇ClN⁺] 338.26).

Bacterial Strains

The bacterial strains used in this study are listed in **Table 1**. All the strains, apart from *E. faecalis*, were stored at the Department of Epidemiology, Faculty of Military Health Sciences, University of Defence in Brno (Czechia) using ITEST CRYOBANK B cryotubes (ITEST plus s.r.o., Hradec Kralove, Czechia) in a freeze box at -70°C . Before MIC/MBC testing by broth microdilution method, all strains were cultivated on Mueller-Hinton agar (HiMedia, Cadersky-Envitek, Prague, Czechia). *Enterococcus faecalis* DSM 16431 (kindly donated by SymbioGruppe GmbH & Co KG SymbioPharm GmbH) was stored in cryovials at the Department of Microbiology, Biotechnical Faculty, University of

TABLE 1 | Bacterial strains used in this study.

	Strain	Abb. ^a	Source
G+	<i>Staphylococcus aureus</i> C1947	STAU	Clinical isolate ^b
	methicillin-resistant <i>S. aureus</i> C1926	MRSA	Clinical isolate ^b
	<i>Staphylococcus epidermidis</i> C1936	STEP	Clinical isolate ^b
	<i>Enterococcus faecalis</i> DSM 16431	EFAE	SymbioGruppe GmbH & Co KG SymbioPharm GmbH)
G–	<i>Escherichia coli</i> A1235	ESCO	Clinical isolate ^b
	<i>Klebsiella pneumoniae</i> C1950 extended-spectrum β -lactamase-producing	KLPN–	Clinical isolate ^b
	<i>K. pneumoniae</i> C1934	KLPN+	Clinical isolate ^b

^aabbreviations for Figures and Tables in this publication. ^bclinical isolates of patients from the University Hospital Hradec Kralove.

Ljubljana (Slovenia) and was grown on Tryptic Soy Agar (Biolife, Italiana S.r.l., Milan, Italy).

Planktonic Bacteria Susceptibility Assay

The antibacterial susceptibility of planktonic bacteria was determined by the broth microdilution method according to the standard M07-A1 (CLSI, 2018) and optimized as described previously (Marek et al., 2015; Dolezal et al., 2016). All antibacterial compounds were dissolved in dimethyl sulfoxide (DMSO p.a., Sigma-Aldrich, Prague, Czechia). The wells of the 96-well microtiter plates contained 200 μ L of Mueller-Hinton broth (MHB, HiMedia, Cadersky-Envitek, Prague, Czechia) with two-fold serial dilutions of the QACs (500–0.49 μ mol/L) and were inoculated with 10 μ L of exponentially grown bacterial suspension adjusted densitometrically to match 0.5 McFarland scale. The final concentrations of DMSO in broth did not exceed 1%. The MIC values, defined as inhibition of bacterial growth, were determined visually after 24 and 48 h of incubation at $35^{\circ}\text{C} \pm 1^{\circ}\text{C}$. The MBCs were determined for all prepared compounds as the concentrations that provided $\geq 99.9\%$ decrease in the bacterial number after subculture of 10 μ L aliquots from each microtiter well in a corresponding new microtiter plate where each well contained 200 μ L of fresh MHB. The MBC was determined as the lowest concentration which corresponded to a well without visible bacterial growth after a further 24 h of incubation at $35 \pm 1^{\circ}\text{C}$. To ensure that no bacteria had survived, the content of the well was inoculated on an agar plate to confirm the absence of bacterial growth.

To evaluate the effect of bacterial density on the antibacterial activity of the QACs, *E. faecalis* suspensions from an overnight culture were prepared in the range from 10^6 to 10^{10} CFU/mL in Brain Heart Infusion broth (BHI, VWR International BVBA, Leuven, Belgium) by either diluting or concentrating bacterial suspensions. The MBCs corresponding to *E. faecalis* suspensions with different initial bacterial densities were determined only for the compound A₁₄ in the concentration range between 500 and 0.49 μ M prepared by 2-fold serial dilutions. The MBCs were evaluated as described above after the bacteria were exposed to

the QACs for 3 min, 60 min or 24 h. The growth rate of tested *E. faecalis* suspensions at different initial bacterial densities was monitored every 30 min during 7 h of incubation by measuring the optical density (OD_{600}). The values were fitted with the logistic equation

$$N(t) = \frac{KN_0}{(K - N_0)e^{-rt} + N_0}$$

where N_0 is the initial OD_{600} , K is the carrying capacity (maximal OD_{600} in the stationary growth phase), t is the length of time of incubation, and r is the growth rate constant.

Biofilm Susceptibility Assay

To grow the biofilms, an overnight culture of *E. faecalis* (average viable bacterial concentration of 1×10^8 CFU/ml) was diluted 100-fold in BHI. *E. faecalis* biofilms were formed on titanium radial disks (commercially pure titanium, grade 2) with 7 mm diameter and 1 mm thickness. Prior to the experiments all disks were sandblasted (FerroEcoBlast Europe; Microblast ceramic beads B120) to expose fresh titanium surface, cleaned in 70% ethanol and autoclaved at 134°C for 20 min. The biofilms were grown for 3 days at 37°C \pm 1°C without shaking or changing of media to achieve a surface coverage of approximately 25% and a surface bacterial density of $\sim 1.5 \times 10^{11}$ bacteria per mL. Biofilms grown on a titanium surface were exposed to 1.5 ml of **A**₁₄, **B**₁₄, and **C**₁₄ dissolved in BHI for 1, 3, and 60 min. After treatment the individual disks were rinsed with saline solution to remove QACs as well as unattached bacteria. In laser treated biofilms samples were treated with QACs for 1 min followed by 10 s of Er:YAG – SSP laser treatment. The LightWalker Er:YAG (Fotona, Ljubljana, Slovenia) was set with the following parameters: laser wavelength 2940 nm; contact handpiece H14, Flat Sweeps fiber tip 400/14 positioned 5 mm above the biofilm disk, energy 20 mJ, frequency 15 Hz, water off, air off, single pulse modality – SSP (super short pulse – 50 μ s). The titanium disks with their biofilm were positioned at the bottom of cylindrical irrigation system (7.5 mm diameter and 2 cm high) in the presence of 1.5 ml of either saline or the QAC dissolved in BHI. The antibacterial concentration was 250 μ M which was the highest soluble QAC concentration in BHI broth. The rinsed biofilms were stained with 5 μ L of premixed saline-diluted Syto 9 and propidium iodide stock solutions (1: 300) from LIVE/DEAD™ BacLight™ Bacterial Viability Kit L7012 (Thermo Fisher Scientific, Eugene, OR, United States). After 5 min of incubation in the dark the samples were observed by fluorescence microscope Zeiss Axio Observer Z1 equipped with confocal unit LSM 800 (CLSM). Z-stacks and tiles were taken at 100 \times or 20 \times magnification at three randomly selected view fields. Image acquisition and control of the microscope were performed with ZEN 2.3 (ZEISS GmbH, Germany). For the 100 \times magnification, blue 488 nm and yellow 561 nm lasers were set to 1% intensity, GaAsP PMT detectors to 700 V, pinhole to 71 μ m, and the size of the acquired 8-bit images was 3476 \times 3476 pixels. For the 20 \times magnification, blue 488 nm and yellow 561 nm lasers were set to 0.85% intensity, GaAsP PMT detectors to 700 V, pinhole to 50 μ m and the size of acquired 8-bit images was 1306 \times 1306 pixels. The typical Z-step of the Z-stack was 1 μ m for 100 \times magnification and 3.26 μ m for

20 \times magnification. The images were composed of four different view fields. A custom script was written (Image J) and used to evaluate the effect of treatment on the fraction of dead cells and biofilm surface coverage.

The Bliss independence model was used for the evaluation of interactions of the combined QACs and laser treatment (Bliss, 1939). The model assumes that a single agent acts independently but contributes to the final outcome (Bliss, 1939; Foucquier and Guedj, 2015). The observed combined effect (E_{obs}) is compared to the expected combined effect (E_{exp}) which is calculated as $E_{exp} = 1 - (1 - E_1) \times (1 - E_2)$, where E_1 and E_2 are the effects of the single treatments. The difference between the E_{obs} and E_{exp} is the Excess over Bliss (*eob*). Positive *eob* values indicate synergistic interaction, whereas negative *eob* values indicate antagonistic behavior. Null *eob* value implies no interaction.

Cell Viability Evaluation

Standard MTT assay (3-(4,5-dimethylthiazol-2-yl)-2,5-diphenyltetrazolium bromide; Sigma-Aldrich, Prague, Czechia) was used according to the manufacturer's protocol on the CHO-K1 (Chinese hamster ovary, ECACC, Salisbury, United Kingdom) in order to compare the effect of different compounds within the series. The cells were cultured according to ECACC recommended conditions and seeded in a density of 8000 per well as described previously (Soukup et al., 2020). Briefly, the tested compounds (series A, B, C) were dissolved in DMSO (Sigma-Aldrich, Prague, Czechia) and subsequently diluted in the Nutrient Mixture F-12 Ham growth medium (Sigma-Aldrich, Prague, Czechia) supplemented with 10% Fetal Bovine Serum and 1% Penicillin-Streptomycin (both Sigma-Aldrich, Prague, Czechia) so that the final concentration of DMSO did not exceed 0.5% (v/v). In the case of sodium hypochlorite, the commercially available detergent called Savo containing this active compound was diluted to the initial half concentration (i.e., 2.35%) with the supplemented growth medium mentioned above. Thereafter, CHO-K1 cells were exposed to two-fold diluted series A, B, C or ten-fold diluted sodium hypochlorite for 24 h. Then the medium was replaced by a medium containing 0.5 mg/ml of MTT and the cells were allowed to produce formazan for approximately 3 h under surveillance. Thereafter, the medium with MTT was removed and crystals of formazan were dissolved in DMSO (100 μ l/well). Cell viability was assessed spectrophotometrically by the amount of formazan produced. The absorbance was measured at 570 nm on Synergy HT (BioTek, Winooski, VT, United States). IC_{50} (half maximal inhibitory concentration) was then calculated from the control – subtracted triplicates using non-linear regression (four parameters) by GraphPad Prism 5.03 or 7.03 software (GraphPad Software Inc., San Diego, CA, United States). Final IC_{50} and SEM (standard error of the mean) values were obtained as a mean of three independent measurements.

Statistical Analysis

All biological experiments were independently performed at least three times with three replicates for each sample. The results for the biofilm susceptibility were analyzed by Shapiro–Wilk normality test. Tukey's multiple comparison test was used to

evaluate the live/dead ratio (we have assumed that the data are normally distributed), whereas Dunn's multiple comparison test was used for surface coverage, where the results were not normally distributed. *P*-values of <0.05 were considered to be significant. GraphPad Prism 7.03 software (GraphPad Software Inc., San Diego, CA, United States) was used for statistical analysis and graphical representation.

RESULTS AND DISCUSSION

Chemistry

The chemical structures of 1-Alkylpyridinium derivatives (**A**₁₂, **A**₁₄, **A**₁₆); 1-alkyl-3-chloropyridinium derivatives (**B**₁₂, **B**₁₄, **B**₁₆), and 3-alkyl-1-(2-hydroxyethyl)imidazolium derivatives (**C**₁₂, **C**₁₄, **C**₁₆) are shown in **Figure 1**.

We have prepared 9 quaternary ammonium salts containing pyridine or imidazole heterocyclic rings. The compounds of group A and C were synthesized as described previously and served as reference QACs (Marek et al., 2010; Soukup et al., 2020). The novel antibacterial compounds (B group) were prepared by Menshutkin reaction, where the tertiary amine was converted into a quaternary ammonium salt by reaction with an alkyl halide (nucleophilic substitution-type reaction). Each homologous group consisted of three *N*-alkyl derivatives with either 12, 14 or 16 carbon atoms in the alkyl chain. The structures of the new compounds were confirmed by ¹H and ¹³C NMR and HRMS analysis. The purity of all the compounds was ≥95%. The yields, melting points, purities and Clog *P* (calculated logarithm of the partition coefficient) of different antibacterial compounds are given in **Table 2**. Clog *P* was calculated with MarvinSketch (version 14.9.8.0) software. As expected, the melting points of the new compounds and Clog *P* values increased with increasing alkyl chain length.

In vitro Antibacterial Activity

Susceptibility of QACs Against Planktonic Bacteria

The series of synthesized QACs were evaluated for their antibacterial activity against selected nosocomial planktonic

bacteria using broth microdilution assay. The antibacterial effect of the new chlorine-substituted *N*-Alkylpyridiniums (**B**_{12–16}) and reference *N*-Alkylpyridiniums (**A**_{12–16}) on planktonic bacterial strains is shown in **Figure 2**. All the compounds were effective against the tested bacterial strains. Higher antibacterial activity, as indicated by lower MIC value, was found against the G+ bacteria *E. faecalis* (EFAE), *S. aureus* (STAU), methicillin-resistant *S. aureus* (MRSA), and *S. epidermidis* (STEP). The lowest MIC and MBC values were obtained for *S. aureus*. The observed higher susceptibility of the G+ bacteria to QACs compared to G– bacteria is in agreement with the literature (Tischer et al., 2012; Shtyrlin et al., 2016). There is a general trend of decreasing MIC values with increasing alkyl chain length for all antibacterial compounds tested. The exception is **A**₁₄ which was more efficient against MRSA than **A**₁₆. Such increasing antimicrobial activity with increasing alkyl chain length has been reported previously (Li et al., 2013; Zhang et al., 2016). When an *N*-Alkylpyridinium QAC was compared with a chlorine-substituted *N*-alkylpyridinium or *N*-Alkylimidazolium at a given alkyl chain length (i.e., **A**₁₄, **B**₁₄, and **C**₁₄ in **Figure 2**), there was no significant difference in the antimicrobial activity for G+ bacteria. In the case of the G– bacteria *E. coli* (ESCO), *K. pneumoniae* (KLPN–), and extended-spectrum β-lactamase-producing *K. pneumoniae* (KLPN+), the most effective were imidazolium compounds. Our results are consistent with previous observations that small changes in the structure of QACs such as introduction of electronegative atom allow for fine-tunability of surfactant properties (Brown et al., 2017; Fuente-Nunez et al., 2018).

The Effect of the Initial Bacterial Density on Planktonic Antimicrobial Effectiveness

The effect of different initial bacterial densities on the MBC are given in **Figure 3**. The MBC was determined after 3 min, 60 min, and 24 h of bacterial exposure to the antibacterial compound. The MBC increased with the initial bacterial density. This is usually interpreted as an increased resistance to the antibiotic due to the induction of quorum sensing pathways [i.e., by increasing the number of persistent cells in the population, the expression

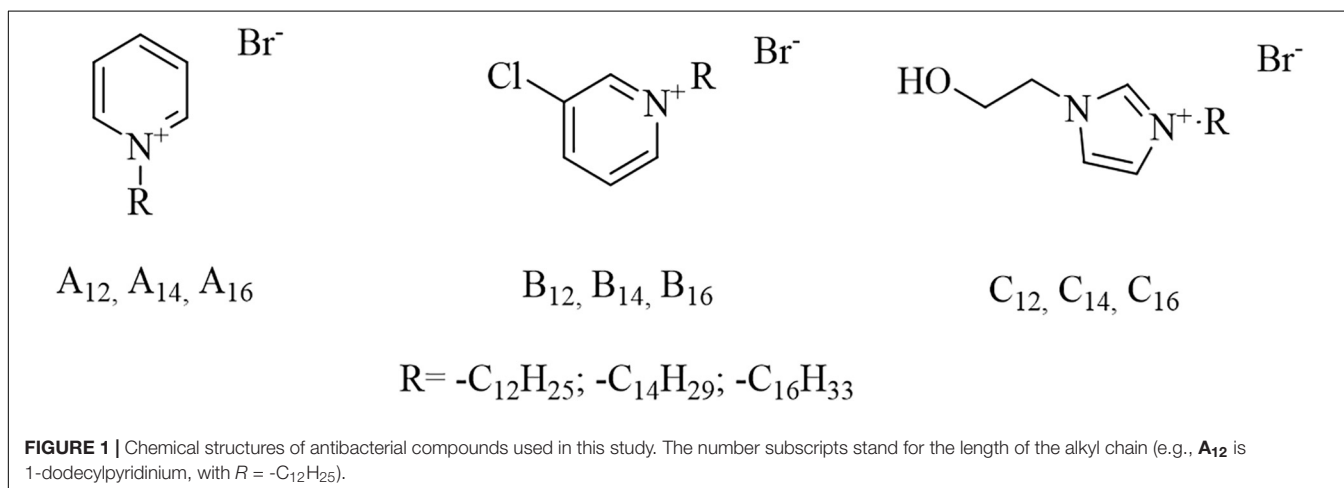
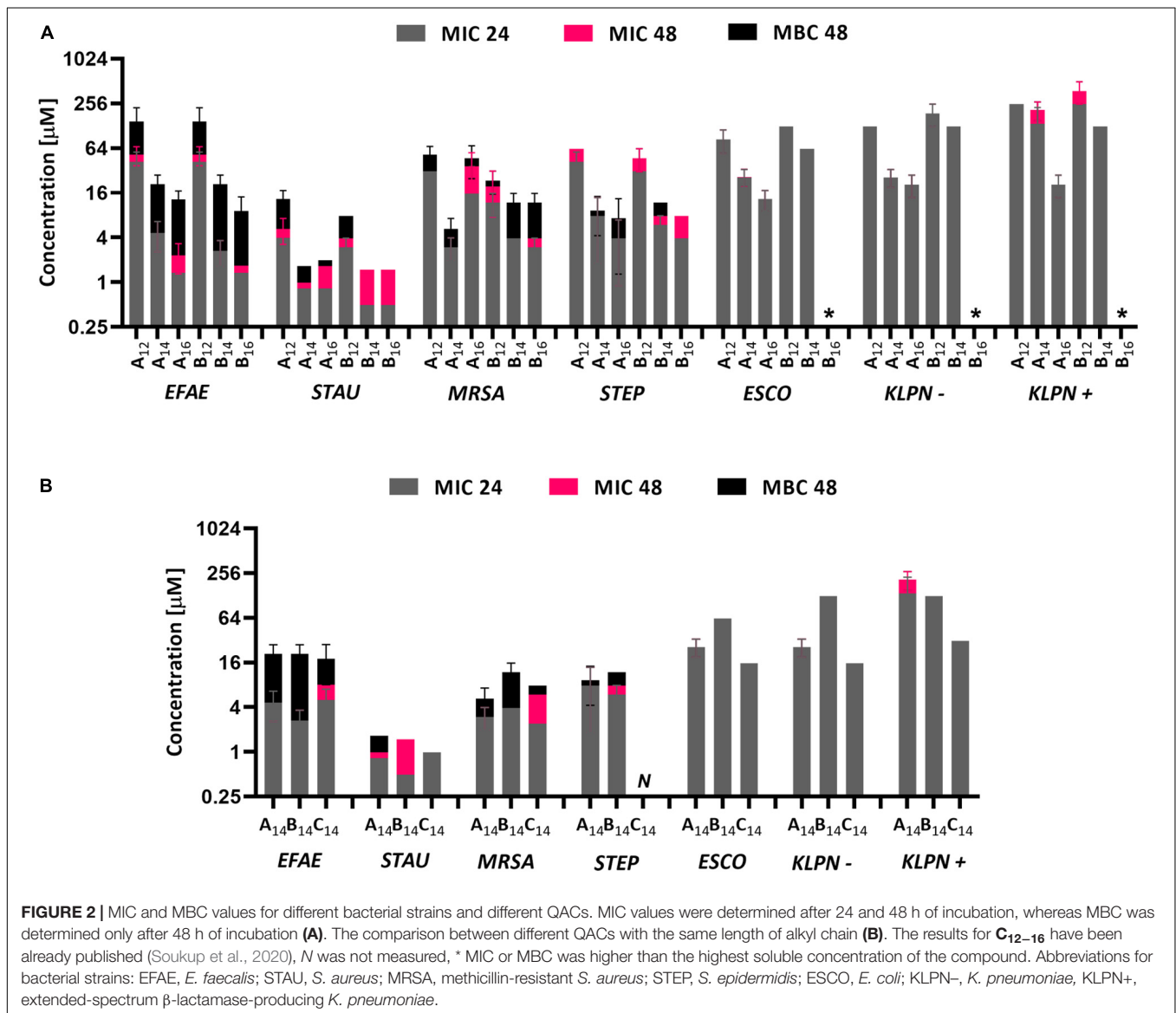


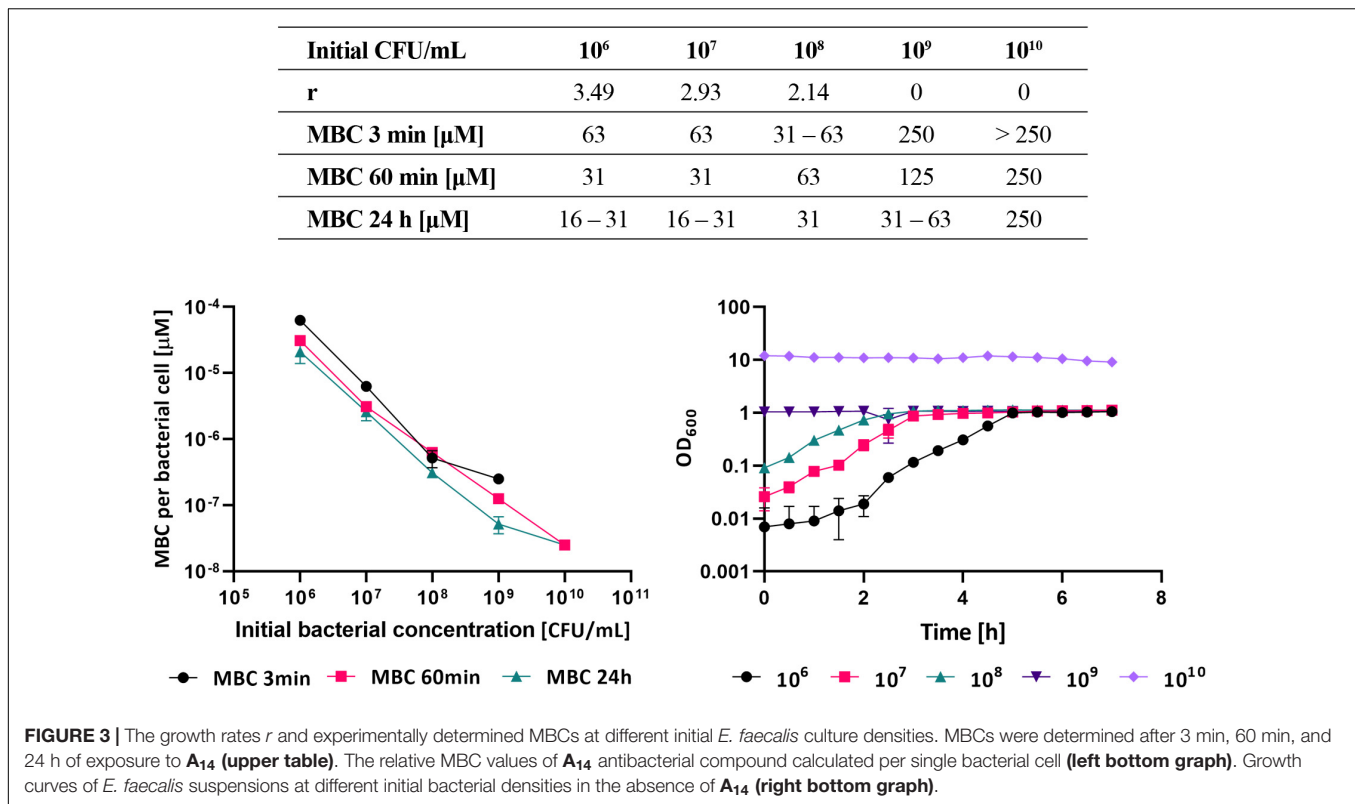
TABLE 2 | Yields, melting points, purity and Clog P of antibacterial QACs used in this study.

Compound	Alkyl chain	Yield (%)	Purity (%)	Melting point (°C)	Clog P
A ₁₂	12	82.13	95	73.0–75.0	1.693
A ₁₄	14	75.61	96	58.0–60.0	2.582
A ₁₆	16	98.76	96	63.0–64.0	3.471
B ₁₂	12	82.84	95	68.5–69.2	2.297
B ₁₄	14	69.27	99	84.0–84.6	3.186
B ₁₆	16	76.53	100	91.4–92.2	4.075
C ₁₂	12	77.76	95	Oil	0.720
C ₁₄	14	83.69	95	44.0–46.0	1.610
C ₁₆	16	17.20	95	49.2–50.1	2.499



of peroxidases which provide protection against reactive oxygen species, or the overexpression of an efflux pump (Rémy et al., 2018)]. The increase in MBC with cell density, however, was

much less than the increase in the number of bacterial cells. If one calculates the relative MBC value per bacterial cell the effective MBC in fact significantly decreases with cell densities (Figure 3).



The required MBC after 24 h at 10⁶ CFU/ml initial bacterial density was 2.1×10^{-5} μM and decreased to 2.7×10^{-8} μM at the initial bacterial density of 10¹⁰ CFU/ml. This is more than three orders of magnitude. The results imply that the denser the initial bacterial suspension the more the individual bacterial cell is susceptible to the antibacterial compound. This is surprising and could be due to an increased level of stress experienced by the individual cell in a more crowded environment. Although at high cell densities bacteria may collectively adapt their behavior and increase antibiotic resistance the results of this study suggest that the individual cells of *E. faecalis* become more stressed and susceptible to the antibiotic at higher initial bacterial concentrations. This could be due to reduced availability of nutrients and reduced growth rate. To check this we have grown bacteria at different initial densities in fresh medium. As illustrated in **Figure 3**, the optical density increased during incubation for the dilute initial bacterial suspensions (i.e., from 10⁶ to 10⁸ CFU/ml), but remained unchanged if the initial bacterial concentration was 10⁹ CFU/ml or higher. The growth rate, which is a general indicator of cell well-being, decreased significantly with increasing initial cell density.

Effectiveness of QACs Against Biofilm

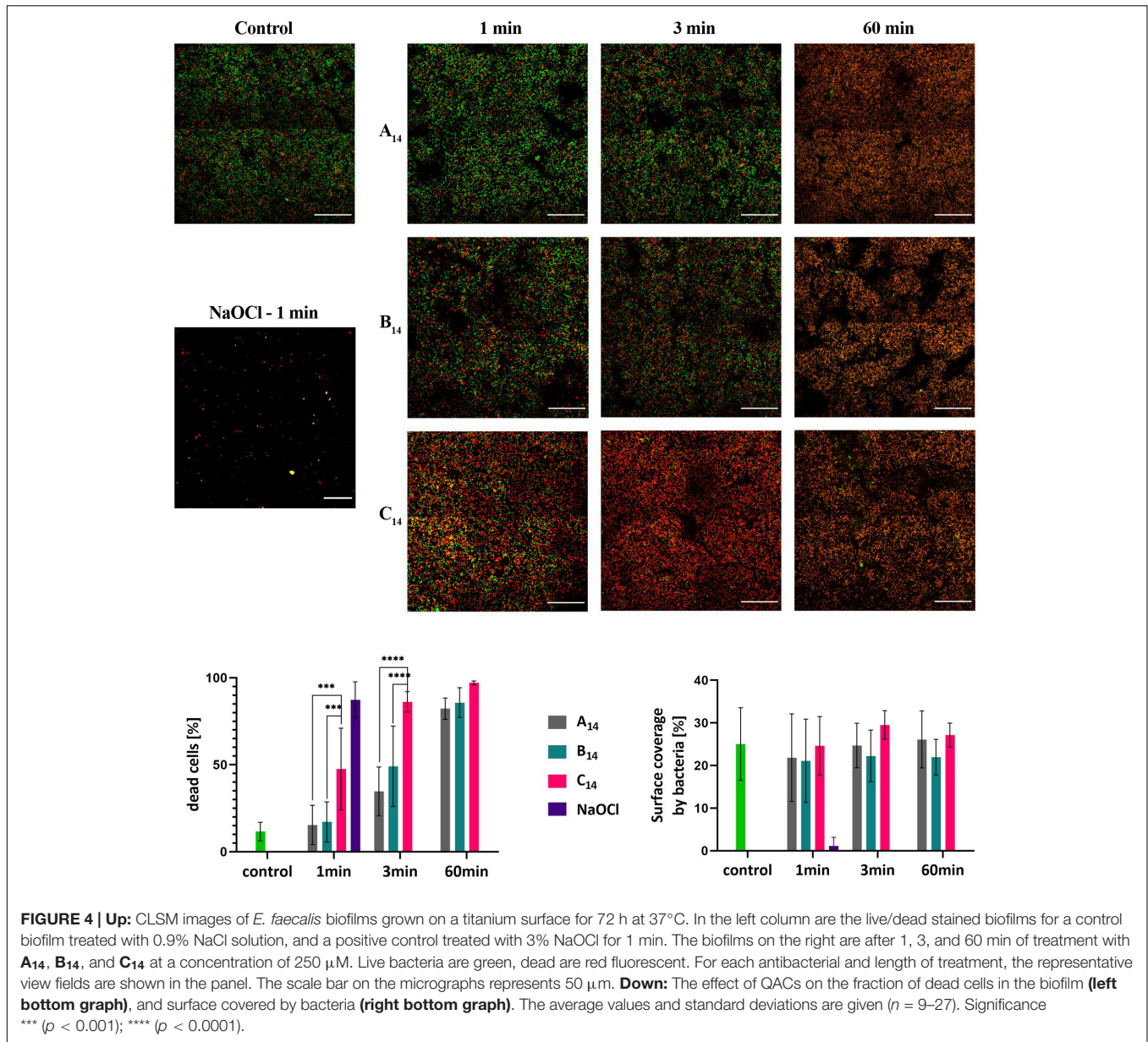
The effectiveness of different QACs against *E. faecalis* biofilms was determined with **A**₁₄, **B**₁₄, and **C**₁₄ compounds as shown in **Figure 4**. All tested QACs were effective against *E. faecalis* biofilms after 60 min of treatment. The fraction of dead (red) cells increased with the time of incubation. The increase was most pronounced for **C**₁₄, where the majority of cells in the biofilm

were dead already after 1 min of treatment. The effectiveness of **B**₁₄ was higher than that of **A**₁₄. As a positive control we have used Sodium hypochlorite solution applied at the concentration commonly used in clinical practice (3% V/V). After 1 min of exposure the biofilm coverage decreased below 1%. The applied NaOCl concentration was approximately 150 times higher than QACs' concentrations used in this study.

To quantify the effect of different QACs on *E. faecalis* biofilms we have determined the fraction of dead cells and the biofilm surface coverage prior to and after the treatment (**Figure 4**). Prior to treatment, most of the bacterial cells in a biofilm ($88 \pm 6\%$) were alive. After 60 min of treatment, the proportions of live cells decreased dramatically and were 18, 14, and 3% for **A**₁₄, **B**₁₄, and **C**₁₄, respectively. The most effective compound against biofilm bacteria was **C**₁₄, where after 3 min of treatment the fraction of dead bacteria was already $86 \pm 4\%$. **B**₁₄ was more effective than **A**₁₄. It is interesting to note that surface coverage did not change significantly during the treatment, suggesting that **A**₁₄, **B**₁₄, and **C**₁₄ kill bacterial cells in a biofilm, but do not remove them from the surface. Similar behavior has been observed for chlorhexidine treatment, where the bacteria in the biofilm were killed, but not removed from the dentin surface (Paz et al., 2010).

Comparison of the Effectiveness of QACs Against Planktonic and Biofilm Cells

In plankton suspensions we were able to reach bactericidal concentration for all tested QACs. The situation was quite different in biofilms. The concentrations that work in plankton were not sufficient to kill all bacteria in the biofilm. It is



usually assumed that antibacterials are significantly less effective in biofilms compared to plankton and up to 1000-fold higher concentrations were reported for biofilms compared to plankton (Ceri et al., 1999; Olson et al., 2002; ASTM International, 2017). Unfortunately, due to the solubility limit, it was not possible to increase the concentration of the QACs to concentrations that would kill all bacteria in the biofilm. Nevertheless, we can compare the effectiveness in plankton and biofilm if we decrease the concentration of biocide in the plankton to match the fraction of the dead cells in the biofilm. The less we have to dilute the concentration of biocide in plankton to match the fraction of dead bacteria in biofilm the more potent the compound is as a biocide in the biofilm. The experiment was performed at high density *E. faecalis* suspensions (2.4×10^9 CFU/mL) to mimic the high density of bacteria in a biofilm. By comparing

QACs effectiveness at high initial planktonic densities we have largely eliminated the effect of the bacterial density and estimated the effect of biofilm induced changes on QACs sensitivity. One has to be careful, however, as bacterial cells in plankton differ from biofilm not only in cell density but also in cell metabolism and extracellular matrix viscoelasticity. To match the fraction of dead cells in the biofilm, the 10-fold dilution of compounds **A₁₄** and **B₁₄** were needed, whereas only 4-fold dilution of compound **C₁₄** was required. This indicates that **C₁₄** has a better activity in the biofilm compared to **A₁₄** and **B₁₄**. The activity of QACs in biofilms relative to plankton was two orders of magnitude lower than usually reported in the literature. Although our biofilms were mature, they were relatively thin (up to 10 μm) which may explain the relatively high efficiency of the QACs against biofilms. Similar observations have been

made for *S. mutans* biofilms, where biofilm cells were only 8 times less susceptible to QACs compared to plankton bacteria (López Pérez et al., 2017).

Er:YAG Photoacoustic Irrigation With QACs in Biofilm Treatment

Although treatment with QACs killed most of the bacteria in biofilms, a significant fraction survived (e.g., 18% with the **A**₁₄ compound after 60 min of treatment). Since 60 min is far too long for many applications (e.g., in dentistry), we tested if laser treatment could potentiate the effect of QACs. To check this we pretreated the biofilms chemically with the QAC for 1 min followed by Er:YAG photoacoustic streaming treatment for 10 s (Figure 5). As a control, biofilms were pretreated with 0.9% NaCl saline solution followed by laser treatment. In the control samples the Er:YAG photoacoustic streaming substantially decreased the biofilm surface coverage, but did not change the fraction of dead bacteria in the biofilms. It is important to note that in photoacoustic streaming with short laser pulses the laser is not acting directly on the surface but it induces cavitation and consequently increases streaming in the fluid, which removes bacteria from the surface but does not change the ratio of live/dead bacteria. On the other hand, when samples were pretreated with QACs followed by laser treatment the fraction of dead cells increased noticeably.

To quantify the data, the proportion of dead cells and the surface coverage after Er:YAG photoacoustic irrigation were determined and are shown in Figure 5. If the cells were in saline solution the laser treatment significantly decreased the surface coverage, but did not significantly change the ratio of live/dead bacteria which remained on the surface. Although the surface coverage decreased more in saline solution compared to QACs the difference was not significant. On the other hands, when biofilms were chemically pretreated with QACs the fraction of dead cells increased significantly after laser treatment, for all tested QACs. To check if the potentiation provided by laser treatment is synergistic or additive, we have determined the Bliss independence index. In all cases it was positive indicating a synergistic action of QACs and laser treatment. The synergistic effect was most pronounced with the novel **B**₁₄. Taken together, these data imply that short laser treatment dramatically improves the effectiveness of QACs by removing bacteria from the surface and by increasing the killing rate. This may allow a shorter chemical exposure time and lower dosage of QACs used in applications.

Cytotoxicity of QACs

In vitro cytotoxicity evaluation of QACs on mammalian CHO-K1 (Chinese hamster ovary) cell line is given in Table 3. With the increase in the alkyl chain length the cytotoxic potential of the drugs increased. This effect is probably caused due to the increasing lipophilicity expressed as the Clog *P* (Table 2) and correlates most likely with the ability to penetrate into cells more easily (Marek et al., 2015; Soukup et al., 2020).

TABLE 3 | The effect of the tested compounds on the CHO-K1 cell viability.

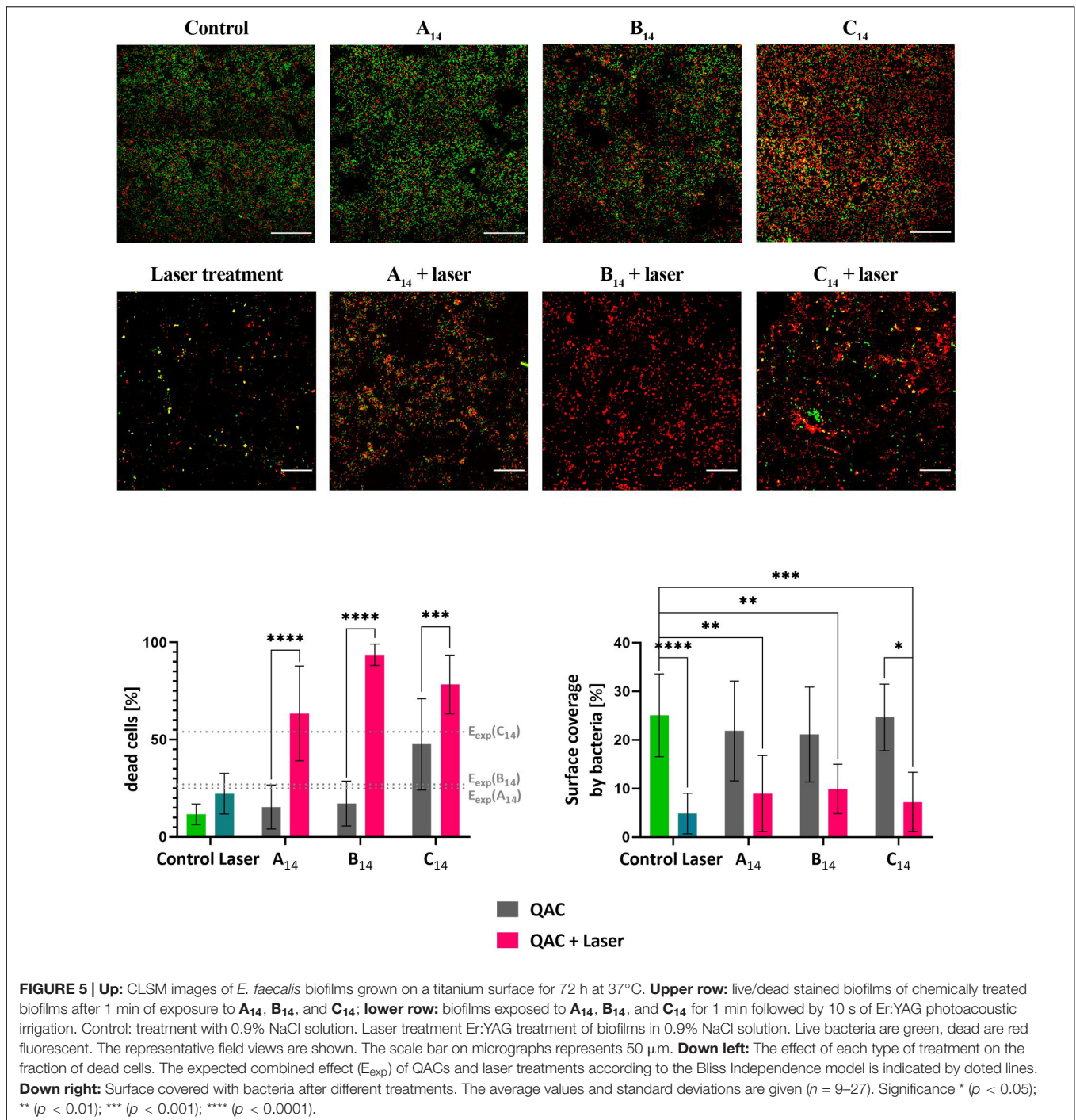
Compound	IC ₅₀ ± SEM (μ M)
A ₁₂ ^a	38.80 ± 0.9
A ₁₄ ^a	24.70 ± 0.2
A ₁₆ ^a	16.70 ± 0.2
B ₁₂	25.50 ± 2.5
B ₁₄	17.17 ± 1.3
B ₁₆	12.54 ± 1.1
C ₁₂ ^b	1.43 ± 3.0
C ₁₄ ^b	1.19 ± 0.9
C ₁₆ ^b	1.03 ± 1.0
Sodium hypochlorite	6.45 ± 1.1

Values are expressed as the IC₅₀: Mean ± SEM (*n* = 3). ^aThe preparation of **A**_{12–16} has been described elsewhere (Marek et al., 2010). ^bThe preparation and the biological assessment of **C**_{12–16} have been described elsewhere (Soukup et al., 2020).

The highest cytotoxicity was determined in the series C which is most likely due to the hydroxyethyl group in the structure. The chlorine substituent in the meta position within the series B caused higher cytotoxicity in comparison to series A. The sodium hypochlorite was more cytotoxic than A and B compounds. The cytotoxicity of commonly used or structure modified QACs was already studied several times. However, the comparison of the obtained values with already published is limited due to the assays' differences, especially regarding to the type of the cells used in experiments. Nevertheless, the cytotoxicity of the well-known QACs representative, benzalkonium chloride, is frequently established in similar range as our QACs [EC₅₀ ~ 12.42 μM for human hepatoma cell line (Christen et al., 2017); IC₅₀ ~ 14.8 μM for Human alveolar cells (Kwon et al., 2019); IC₅₀ ~ 22.8 μM for osteosarcoma cybrid cells (Datta et al., 2017)]. On the other hand, lower toxicity was previously described for QAC-like magnetic and non-magnetic ionic liquid surfactants and their polymeric analogs (~50 μM for human embryonic kidney cells) (Fuente-Nunez et al., 2018).

CONCLUSION

All the selected nosocomial bacterial species were susceptible to the tested QACs in the planktonic state. The novel chlorine substituted *N*-alkylpyridinium (**B**_{12–16}) compounds were most effective against planktonic *S. aureus* with MIC values between 0.5 and 4 μM. The new QACs have an effect comparable to the effect of the non-chlorinated derivatives of *N*-alkylpyridinium and *N*-Alkylimidazolium. The activity of QACs on planktonic bacteria was dependent on the initial bacterial concentration in the suspension. By increasing the initial bacterial concentration, which leads to increased bacterial density during the growth, the level of stress experienced by individual cell was increased. This resulted in lowering the effective QAC concentration needed to kill a bacterial cell. All evaluated QACs demonstrate anti-biofilm activity against *E. faecalis* biofilms grown on a titanium



surface. The best anti-biofilm compound was 3-tetradecyl-1-(2-hydroxyethyl)imidazolium bromide (C₁₄) which was the most cytotoxic. Compared to planktonic bacteria, the biofilm bacteria were only 4-fold more resistant to C₁₄. The most significant finding of this study is that a short 10 s treatment of Er:YAG – SSP photoacoustic steaming irrigation in the presence of new *N*-alkylpyridinium improved significantly its anti-biofilm action. In particular, it decreased the surface coverage of the biofilm and significantly increased the fraction of dead

bacteria. The application of QACs supported by photoacoustic irrigation could be a promising new strategy in combating biofilm-related problems.

DATA AVAILABILITY STATEMENT

The raw data supporting the conclusions of this article will be made available by the authors, without undue reservation.

ETHICS STATEMENT

This study uses strains that were isolated from the samples obtained in the clinical laboratory at the University Hospital Hradec Kralove. The University Hospital Hradec Kralove did not require the study to be reviewed or approved by an Ethics Committee because the clinical strains used in this study come from the routine procedures in the clinical laboratory.

AUTHOR CONTRIBUTIONS

MH performed biological experiments, result analysis, conducted the work and was involved in the designing of the work, writing and interpretation of the data. ST was participating on biological experiments, designing of the work, writing and interpretation of the data. AM performed synthesis and participated in writing. LPr performed NMR and HPLC analysis. LPu performed cytotoxicity experiments. MB participate in writing and interpretation of the data. ID was involved in CSLM imaging, data analysis and writing. JM participated in synthesis, writing and interpretation of the data. DS was involved in designing of the work, writing, interpretation of the data and submission of the manuscript.

REFERENCES

- Akçay, M., Arslan, H., Mese, M., Durmus, N., and Capar, I. D. (2017). Effect of photon-initiated photoacoustic streaming, passive ultrasonic, and sonic irrigation techniques on dentinal tubule penetration of irrigation solution: a confocal microscopic study. *Clin. Oral Investig.* 21, 2205–2212. doi: 10.1007/s00784-016-2013-y
- ASTM International (2017). *ASTM E2799-17, Standard Test Method for Testing Disinfectant Efficacy Against Pseudomonas aeruginosa Biofilm using the MBEC Assay*. West Conshohocken, PA: ASTM International.
- Bliss, C. I. (1939). The toxicity of poisons applied jointly. *Ann. Appl. Biol.* 26, 585–615. doi: 10.1111/j.1744-7348.1939.tb06990.x
- Boutsioukis, C., Verhaagen, B., Versluis, M., Kastrinakis, E., Wesselink, P. R., and van der Sluis, L. W. M. (2010). Evaluation of irrigant flow in the root canal using different needle types by an unsteady computational fluid dynamics model. *J. Endod.* 36, 875–879. doi: 10.1016/j.joen.2009.12.026
- Brown, P., Sresht, V., Eral, B. H., Fiore, A., Fuente-Núñez, C., O'Mahony, M., et al. (2017). CO₂-reactive ionic liquid surfactants for the control of colloidal morphology. *Langmuir* 33, 7633–7641. doi: 10.1021/acs.langmuir.7b00679
- Ceri, H., Olson, M. E., Stremick, C., Read, R. R., Morck, D., and Buret, A. (1999). The Calgary biofilm device: new technology for rapid determination of antibiotic susceptibilities of bacterial biofilms. *J. Clin. Microbiol.* 37, 1771–1776. doi: 10.1128/jcm.37.6.1771-1776.1999
- Christen, V., Faltermann, S., Brun, N. R., Kunz, P. Y., and Fent, K. (2017). Cytotoxicity and molecular effects of biocidal disinfectants (quaternary ammonia, glutaraldehyde, poly(hexamethylene biguanide) hydrochloride PHMB) and their mixtures in vitro and in zebrafish eleuthero-embryos. *Sci. Total Environ.* 586, 1204–1218. doi: 10.1016/j.scitotenv.2017.02.114
- Clarkson, R. M., and Moule, A. J. (1998). Sodium hypochlorite and its use as an endodontic irrigant. *Aust. Dent. J.* 43, 250–256. doi: 10.1111/j.1834-7819.1998.tb00173.x
- CLSI (2018). *Methods for Dilution Antimicrobial Susceptibility Tests for Bacteria that Grow Aerobically: CLSI Standard M07*, 11th Edn. Wayne, PA: Clinical and Laboratory Standards Institute.
- Courvalin, P. (2016). Why is antibiotic resistance a deadly emerging disease? *Clin. Microbiol. Infect.* 22, 405–407. doi: 10.1016/j.cmi.2016.01.012

FUNDING

This work was supported by the Lifelong Learning Programme/ERASMUS of the European Commission, which allowed a working collaboration between the research groups at the University of Defence in Brno and the University of Ljubljana. We would like to acknowledge the financial support from the Slovenian Research Agency (research core funding P4-0116) and Ministry of Health of the Czech Republic (project NV 19-09-00198), Ministry of Education, Youth and Sports of the Czech Republic (project SV/FVZ201905), and Faculty of Military Health Sciences (Long-term development plan). The *E. faecalis* DSM 16431 was provided by SymbioGruppe GmbH & Co KG SymbioPharm GmbH). The titanium disks and Er:YAG laser system was provided by Fotona d.o.o., Ljubljana. The microscopy was supported by the University infrastructural center “Microscopy of biological samples” located in Biotechnical Faculty, University of Ljubljana.

ACKNOWLEDGMENTS

The authors are grateful to Ian McColl MD, Ph.D. for assistance with the manuscript.

- Datta, S., Baudouin, C., Brignole-Baudouin, F., Denoyer, A., and Cortopassi, G. A. (2017). The eye drop preservative benzalkonium chloride potently induces mitochondrial dysfunction and preferentially affects LHON mutant cells. *Investig. Ophthalmology Vis. Sci.* 58:2406. doi: 10.1167/iovs.16-20903
- Dolezal, R., Soukup, O., Malinak, D., Savedra, R. M. L., Marek, J., Dolezalova, M., et al. (2016). Towards understanding the mechanism of action of antibacterial N-alkyl-3-hydroxypyridinium salts: biological activities, molecular modeling and QSAR studies. *Eur. J. Med. Chem.* 121, 699–711. doi: 10.1016/j.ejmech.2016.05.058
- Fouquier, J., and Guedj, M. (2015). Analysis of drug combinations: current methodological landscape. *Pharmacol. Res. Perspect.* 3:e00149. doi: 10.1002/prp2.149
- Fuente-Nunez, C., Brown, P., Torres, M. D. T., Cao, J., and Lu, T. K. (2018). Magnetic surfactant ionic liquids and polymers with tetrahaloferrate (III) anions as antimicrobial agents with low cytotoxicity. *Colloid Interface Sci. Commun.* 22, 11–13. doi: 10.1016/j.colcom.2017.11.002
- Gerba, C. P. (2015). Quaternary ammonium biocides: efficacy in application. *Appl. Environ. Microbiol.* 81, 464–469. doi: 10.1128/AEM.02633-14
- Jennings, M. C., Ator, L. E., Paniak, T. J., Minbiole, K. P. C., and Wuest, W. M. (2014). Biofilm-eradicating properties of quaternary ammonium amphiphiles: simple mimics of antimicrobial peptides. *ChemBioChem* 15, 2211–2215. doi: 10.1002/cbic.201402254
- Khan, H. A., Baig, F. K., and Mehboob, R. (2017). Nosocomial infections: epidemiology, prevention, control and surveillance. *Asian Pac. J. Trop. Biomed.* 7, 478–482. doi: 10.1016/j.apjtb.2017.01.019
- Kurzmann, C., Meire, M. A., Lettner, S., Farmakis, E. T. R., Moritz, A., and De Moor, R. J. G. (2019). The efficacy of ultrasonic and PIPS (photon-induced acoustic streaming) irrigation to remove artificially placed dentine debris plugs out of an artificial and natural root model. *Lasers Med. Sci.* 35, 719–728. doi: 10.1007/s10103-019-02912-3
- Kwon, D., Lim, Y., Kwon, J., Shim, I., Kim, E., Lee, D., et al. (2019). Evaluation of pulmonary toxicity of benzalkonium chloride and triethylene glycol mixtures using in vitro and in vivo systems. *Environ. Toxicol.* 34, 561–572. doi: 10.1002/tox.22722
- Li, F., Weir, M. D., and Xu, H. H. K. (2013). Effects of quaternary ammonium chain length on antibacterial bonding agents. *J. Dent. Res.* 92, 932–938. doi: 10.1177/0022034513502053

- López Pérez, D., Baker, P. J., Pintar, A. L., Sun, J., Lin, N. J., and Lin-Gibson, S. (2017). Experimental and statistical methods to evaluate antibacterial activity of a quaternary pyridinium salt on planktonic, biofilm-forming, and biofilm states. *Biofouling* 33, 222–234. doi: 10.1080/08927014.2017.1286476
- Lukač, N., and Jezeršek, M. (2018). Amplification of pressure waves in laser-assisted endodontics with synchronized delivery of Er:YAG laser pulses. *Lasers Med. Sci.* 33, 823–833. doi: 10.1007/s10103-017-2435-z
- Marek, J., Malinak, D., Dolezal, R., Soukup, O., Pasdiorova, M., Dolezal, M., et al. (2015). Synthesis and disinfection effect of the pyridine-4-aldoxime based salts. *Molecules* 20, 3681–3696. doi: 10.3390/molecules20033681
- Marek, J., Stodulka, P., Cabal, J., Soukup, O., Pohanka, M., Korabecny, J., et al. (2010). Preparation of the pyridinium salts differing in the length of the N-Alkyl substituent. *Molecules* 15, 1967–1972. doi: 10.3390/molecules15031967
- Olivi, G., DiVito, E., Peters, O., Kaitsas, V., Angiero, F., Signore, A., et al. (2014). Disinfection efficacy of photon-induced photoacoustic streaming on root canals infected with *Enterococcus faecalis*. *J. Am. Dent. Assoc.* 145, 843–848. doi: 10.14219/jada.2014.46
- Olson, M. E., Ceri, H., Morck, D. W., Buret, A. G., and Read, R. R. (2002). Biofilm bacteria: formation and comparative susceptibility to antibiotics. *Can. J. Vet. Res.* 66, 86–92.
- Paz, L. E. C., Bergenholtz, G., and Svensäter, G. (2010). The effects of antimicrobials on endodontic biofilm bacteria. *J. Endod.* 36, 70–77. doi: 10.1016/j.joen.2009.09.017
- Rémy, B., Mion, S., Plener, L., Elias, M., Chabrière, E., and Daudé, D. (2018). Interference in bacterial quorum sensing: a biopharmaceutical perspective. *Front. Pharmacol.* 9:203. doi: 10.3389/fphar.2018.00203
- Shtyrlin, N. V., Sapozhnikov, S. V., Galiullina, A. S., Kayumov, A. R., Bondar, O. V., Mirchink, E. P., et al. (2016). Synthesis and antibacterial activity of quaternary ammonium 4-deoxy pyridoxine derivatives. *BioMed Res. Int.* 2016:3864193. doi: 10.1155/2016/3864193
- Soukup, O., Benkova, M., Dolezal, R., Sleha, R., Malinak, D., Salajkova, S., et al. (2020). The wide-spectrum antimicrobial effect of novel N-alkyl monoquaternary ammonium salts and their mixtures; the QSAR study against bacteria. *Eur. J. Med. Chem.* 206:112584. doi: 10.1016/j.ejmech.2020.112584
- Tischer, M., Pradel, G., Ohlsen, K., and Holzgrabe, U. (2012). Quaternary ammonium salts and their antimicrobial potential: targets or nonspecific interactions? *ChemMedChem* 7, 22–31. doi: 10.1002/cmdc.201100404
- Watkins, K. (2018). Emerging infectious diseases: a review. *Curr. Emerg. Hosp. Med. Rep.* 6, 86–93. doi: 10.1007/s40138-018-0162-9
- Zehnder, M. (2006). Root canal irrigants. *J. Endod.* 32, 389–398. doi: 10.1016/j.joen.2005.09.014
- Zhang, K., Cheng, L., Weir, M. D., Bai, Y.-X., and Xu, H. H. (2016). Effects of quaternary ammonium chain length on the antibacterial and remineralizing effects of a calcium phosphate nanocomposite. *Int. J. Oral Sci.* 8, 45–53. doi: 10.1038/ijos.2015.33
- Zhang, Y., Chen, Y., Hu, Y., Huang, F., and Xiao, Y. (2018). Quaternary ammonium compounds in dental restorative materials. *Dent. Mater. J.* 37, 183–191. doi: 10.4012/dmj.2017-096

Conflict of Interest: The authors declare that the research was conducted in the absence of any commercial or financial relationships that could be construed as a potential conflict of interest.

Copyright © 2020 Hympanova, Terlep, Markova, Prchal, Dogsa, Pulkrabkova, Benkova, Marek and Stopar. This is an open-access article distributed under the terms of the Creative Commons Attribution License (CC BY). The use, distribution or reproduction in other forums is permitted, provided the original author(s) and the copyright owner(s) are credited and that the original publication in this journal is cited, in accordance with accepted academic practice. No use, distribution or reproduction is permitted which does not comply with these terms.